Kragujevac J. Sci. 46 (2024) 45-57
doi: 10.5937/KgJSci2401045D

UDC 544.537:544.538:544.431.143
Original scientific paper

ADIABATIC RESPONSE OF $3s_2 \rightarrow 2p_4$ AND $3s_3 \rightarrow 2p_5$ NEON TRANSITIONS TO LASER FIELD VARIATIONS

Hristina S. Delibašić Marković[1,*], Violeta M. Petrović[1], Ivan D. Petrović[2]

[1]*University of Kragujevac, Faculty of Science, Radoja Domanovića 12, 34000 Kragujevac, Serbia*
[2]*Academy of Professional Studies Šumadija, Department in Kragujevac, Kosovska 8, 34000 Kragujevac, Serbia*
*****Corresponding author; E-mail: hristina.delibasic@pmf.kg.ac.rs

(Received March 03, 2024; Accepted May 19, 2024)

ABSTRACT. In this research, we delve into the ionization dynamics of neon, focusing on the transitions $3s_2 \rightarrow 2p_4$ and $3s_3 \rightarrow 2p_5$. Employing the Landau-Dykhne approximation, we elucidate how variations in laser intensity, atomic charge, and wavelength influence the ionization rates. Our study unveils a detailed dependency of the ionization process on these laser parameters, affirming the laser's pivotal role in atomic excitations. We discover that while the ionization rates are markedly affected by laser intensity and atomic charge, wavelength variations also significantly alter the transition dynamics. This work emphasizes the minimal impact of relativistic effects in neon, thereby establishing it as an excellent system for examining laser-atom interaction nuances. Our findings provide valuable insights into the quantum mechanical underpinnings of laser-induced ionization, enhancing the theoretical framework and informing future experimental inquiries into such interactions.

Keywords: transition amplitude, ionization rate, laser parameters.

INTRODUCTION

The evolution of laser technology over the past decades has not only revolutionized our understanding of the interplay between laser fields and atomic and molecular systems but has also unraveled the complexities of the ionization processes (PETROVIĆ *et al*., 2023; BORREGO-VARILLAS *et al*., 2022; PETERS, 2021). These advancements have propelled theoretical physics into new frontiers, notably in applied sciences, such as laser-induced breakdown (LIB) and the precise manipulation of free-electron densities (DELIBASIC *et al*., 2020; ZHANG and YANG, 2020). A pivotal aspect of this scientific journey is the nuanced comprehension of ionization rates, a fundamental parameter that significantly affects the dynamics of free electron densities

ORCID ID:
H. Delibašić Marković - 0000-0002-8391-4179; V.M. Petrović - 0000-0002-7865-523X;
I.D. Petrović - 0009-0003-2419-8787.

and, consequently, influences the optical and physical properties of materials subjected to laser irradiation. At the core of this area of study lie the seminal contributions of Landau and Lifshitz (LANDAU and LIFSHITZ, 2013), who laid the initial theoretical groundwork for atomic ionization within electromagnetic fields. This foundational work set the stage for the landmark contributions of Keldysh, who introduced a model that categorized ionization mechanisms into tunnel ionization (TI) for $\gamma \ll 1$ and multiphoton ionization (MPI) for $\gamma \gg 1$ (KELDYSH, 1965). The Keldysh parameter γ thus emerged as a critical factor in bridging these ionization regimes. Keldysh's model has been pivotal in deepening our understanding of the response of atoms and molecules to varying laser intensities, facilitating a broader exploration into the dynamics of nonlinear photoionization. Building upon this theoretical foundation, the Perelomov-Popov-Terent'ev (PPT) model (PERELOMOV *et al.*, 1966) introduced substantial refinements by meticulously incorporating the effects of Coulomb interactions and the impact of variably polarized laser fields. This refined approach has been important in providing a more intricate and accurate depiction of ionization dynamics, closely aligning with experimental data, and enriching our theoretical tools for examining laser-matter interactions. Concurrently, the development of the Ammosov-Delone-Krainov (ADK) theory (AMMOSOV *et al.*, 1986) presented an alternative methodology for assessing ionization rates, particularly within the tunnel ionization regime for complex atoms and ions. Despite its limitations under specific scenarios, the ADK model's simplicity and practicality have cemented its importance in theoretical considerations, enabling a pragmatic evaluation of ionization processes across various laser intensities.

Central to the theoretical exploration of ionization dynamics is the Landau-Dykhne adiabatic approximation (DYKHNE, 1962), a concept that has significantly influenced the field by offering a robust method for calculating transition probabilities in quantum systems subjected to slowly varying external fields. This approximation, integral to our understanding of adiabatic processes, underpins the theoretical analysis of ionization rates, especially in the context of strong-field ionization. By employing this approximation, we gain valuable insights into the adiabatic nature of electron dynamics, allowing for a more comprehensive understanding of ionization mechanisms under high-intensity laser fields. The Landau-Dykhne approximation forms the cornerstone of our theoretical investigation in this paper, enabling a detailed analysis of ionization rates and contributing to the broader discourse on laser-matter interaction dynamics.

In this study, our paper aims to contribute to the field by presenting a theoretical framework specifically designed to calculate the ionization rate for the $3s_2 \rightarrow 2p_4$ and $3s_3 \rightarrow 2p_5$ transitions of neon (Ne) atoms under adiabatic perturbations. This work, which situates itself within the broader discourse initiated by predecessors like Landau and Dykhne, seeks to elucidate the role of laser intensity and wavelength in strong-field ionization, while also considering the impact of additional ionization processes on the transition rate. Our findings not only engage with the established theoretical framework but also offer new insights, particularly highlighting the non-relativistic domain where magnetic field effects are negligible - a distinction that sets our work apart and provides a nuanced understanding of ionization dynamics influenced predominantly by the electric component of the laser field.

This paper presents a methodical investigation of the ionization dynamics in neon, focusing on the $3s_2 \rightarrow 2p_4$ and $3s_3 \rightarrow 2p_5$ transitions. Our manuscript is organized into distinct sections for clarity and depth of analysis. The section "Theoretical Framework" lays out the foundations of our study, where we derive the ionization rate equations for the neon transitions using the adiabatic Landau-Dykhne approximation. This is followed by "Results and Discussion," where we analyze our theoretical findings, shedding light on the nuances of atomic response to laser manipulation. Finally, in "Conclusion," we synthesize our insights, reflect on the significance of our research within the broader context of atomic physics, and outline potential directions for future research.

Theoretical framework

In the framework of quantum mechanics, the analysis of a two-level Hamiltonian system under the adiabatic approximation is a fundamental approach to understanding how quantum states evolve when subjected to slowly varying external conditions. This approximation allows us to explore the system's dynamics through its energy eigenvalues, $E_j(t)$, which are solutions to the Schrödinger equation, $\mathrm{H(t)}\,\Psi_j(t) = E_j(t)\,\Psi_j(t)$ (MILOŠEVIĆ *et al.*, 2022). Here, $\mathrm{H(t)}$ represents the time-dependent Hamiltonian of the system, and $\Psi_j(t)$ denotes the eigenfunctions corresponding to each energy eigenvalue. The physical picture becomes clearer when we express the eigenfunctions as $\Psi_j(t) \propto \mathrm{Exp}[-i \int E_j(t')\,dt']$. This expression encapsulates the phase evolution of the quantum state over time, where the integral of the energy eigenvalue over time gives the phase accumulated by the state. Such a representation is crucial for understanding the coherence properties of quantum states and their temporal evolution under the influence of external forces.

The concept of transition amplitudes, A_{mn}, plays a central role in quantifying the probability amplitude for a system to transition from an initial quantum state n to a final state m due to adiabatic perturbations (DYKHNE, 1962). This transition amplitude is derived by considering the overlap integral between the initial and final state wave functions (Ψ_m^*, Ψ_n), which mathematically represents how much these states 'overlap' or share in common. The calculation of A_{mn} is guided by the equation:

$$A_{mn} = i\,\mathrm{Exp}\left[i \int_{t_1}^{\tau} \omega_{mn}(t)dt\right], \tag{1}$$

where t_1 is any point on the real t −axis and $\omega_{mn}(t)$ denotes transition frequency, defined as $\omega_{mn}(t) = E_m(t) - E_n(t)$, reflecting the energy difference between states m and n, and thereby governing the dynamics of the transition. Furthermore, the parameter τ, a classical turning point in the complex t plane, emerges as a critical factor in the adiabatic approximation. It is defined by the condition $E_n(\tau) = E_m(\tau)$, equating the energies of the initial and final states at the turning point. This turning point is essential for understanding the non-linear dynamics of quantum transitions, particularly in determining the most probable path for a state transition within the complex time plane. Delone and Krainov's insights into selecting the appropriate τ-value (DELONE and KRAINOV, 1998), closest to the real t-axis, underscore the importance of choosing the path that minimizes the action and, hence, maximizes the transition probability. This selection is not merely a mathematical convenience but a profound insight into the physical processes governing quantum transitions under adiabatic conditions. It highlights the interplay between the quantum states and the external environment, elucidating the conditions under which quantum systems exhibit significant transitions.

Building upon the foundational concepts of quantum transitions within the adiabatic framework, we delve further into the specifics of transitioning between quantum states under slowly varying external conditions. The transition from an initial state n to a final state m, pivotal in understanding quantum system dynamics, is quantitatively explored through the adiabatic Landau-Dykhne approximation (DYKHNE, 1962). This approximation is a cornerstone for calculating the ionization rate W_{mn}, which quantifies the probability of a quantum state transitioning from one energy level to another due to adiabatic perturbations and can be derived as:

$$W_{mn} = |A_{mn}|^2 = \mathrm{Exp}\left[-2\,\mathrm{Im}\left\{\int_{t_1}^{\tau} \omega_{mn}(t)dt\right\}\right]. \tag{2}$$

where $|A_{mn}|^2$ signifies the square modulus of the transition amplitude, providing a direct measure of the transition probability. Moreover, Eq. (2) encapsulates the essence of the observed approximation, indicating that the ionization rate is exponentially dependent on the imaginary part of the action integral between states n and m, calculated over a path in the complex time plane from t_1 to τ. It is important to stress that this formulation, as highlighted in Eqs. (1) and (2), is particularly relevant when considering transitions between adjacent quantum levels n and m. However, the scenario becomes more complex with the introduction of a third level positioned between the initial and final states. In such cases, the system faces a choice: a direct transition from n to m or a cascaded transition through the intermediary level. This competition between direct and cascade transitions introduces an additional layer of complexity in calculating ionization rates, as both pathways can significantly influence the overall transition dynamics. The interplay between these transition pathways has been the subject of extensive research (AUGST *et al.*, 1991; TSIBIDIS and STRATAKIS, 2020), revealing that the presence of an intermediate level can either facilitate or inhibit the transition, depending on the system's specifics and the external conditions. This area of study is rich with insights into the mechanisms of quantum transitions, offering a deeper understanding of how quantum systems navigate the landscape of their potential energy states under adiabatic perturbations.

The research presented in this study marks a significant milestone in atomic structure calculations and experimental methodologies. We focus our analysis on the $3s_2 \rightarrow 2p_4$ and $3s_3 \rightarrow 2p_5$ transitions of the Ne atom (Fig. 1), motivated by the aim to calculate the corresponding transition rates and to explore the effects of varying laser intensity and frequency on these rates. The choice of Ne is strategic; for most noble-gas atoms, the lifetimes of the $3s_2$ and $3s_3$ states are significantly influenced by electron correlations and relativistic effects (LILLY and HOLMES, 1968). However, Ne stands out as relativistic corrections have a minimal impact on its atomic transitions, rendering it an ideal candidate for rigorously testing theories of electron correlations.

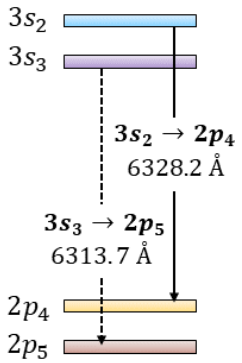

Figure 1. Simplified energy-level scheme for Ne where the $3s_2 \rightarrow 2p_4$ and $3s_3 \rightarrow 2p_5$ transitions are of interest (adapted from LILLY and HOLMES, 1968).

In our theoretical exploration, we subject the $3s_2 \rightarrow 2p_4$ and $3s_3 \rightarrow 2p_5$ transitions (see Fig. 1) to a monochromatic perturbation, represented as $V = V^{(1)}\,\mathrm{Cos}[\omega t] = zF\,\mathrm{Cos}[\omega t]$, where z denotes the atomic charge and F the electric field strength of the laser. This perturbation leads us to the formulation of the Schrödinger equation in the energy representation for the observed two-level system, resulting in the equations:

$$E_n^{(0)} a_n + zF a_m\,\mathrm{Cos}[\omega t] = E_n(t) a_n, \tag{3}$$

$$E_m^{(0)} a_m + zF a_n\,\mathrm{Cos}[\omega t] = E_m(t) a_m. \tag{4}$$

where ω is the angular frequency of the laser field, while $E_n^{(0)}$and $E_m^{(0)}$ represents the unperturbed (or zero-field) energies of the initial, n, and final, m, states, respectively. Those are the energy levels of the atomic system when there is no external electric field applied. Coefficients a_n and a_m are the amplitudes of the quantum states n and m, respectively. They indicate the probability amplitude for finding the system in either state. Finally, $E_n(t)$ and $E_m(t)$ are the instantaneous energies of the states n and m under the influence of the oscillating electric field. Unlike the unperturbed energies $E_n^{(0)}$and $E_m^{(0)}$, these values vary over time as the external field changes. The left-hand side of each equation (see Eqs. (3) and (4)) combine the unperturbed energy of a state with the interaction term that arises due to the external field. The right-hand side relates this combined energy to the time-dependent energy of the state, modulated by the external field's influence. These equations essentially capture the dynamics of quantum states under external perturbations. The presence of the cosine term indicates that the interaction is periodic, leading to the possibility of resonant phenomena when the frequency of the external field matches or comes close to the natural frequencies of the system.

Following the Landau-Dykhne formulation, as detailed in the referenced literature, we adopt the assumption that the zeroth-order energy levels of the states involved in the transition satisfy relation (DYKHNE, 1962): $E_m^{(0)} = -E_n^{(0)} = \omega_{mn}/2 > 0$. This condition implies a symmetrical distribution of energy levels about the zero-energy point, where ω_{mn} represents the energy separation between these levels in the absence of external perturbations. Utilizing this assumption allows us to express the energy eigenvalues $E_n(t)$ and $E_m(t)$, in the presence of an external electric field as:

$$E_m(t) = -E_n(t) = \sqrt{\frac{1}{4}{\omega_{mn}}^2 + |z|^2 F^2 \mathrm{Cos}^2[\omega t]}, \tag{5}$$

which encapsulates the dynamic modulation of the energy levels induced by the oscillating electric field, where the square root term accounts for the combined effect of the static energy separation and the field-induced energy shifts.

The classical turning point, τ, crucial for calculating the transition amplitude, is determined by equating the initial and final energies, $E_n(\tau) = E_m(\tau)$, and employing a Maclaurin series expansion for the $\mathrm{ArcCos}[x] \approx \frac{\pi}{2} - x - \cdots$ (GUO *et al.*, 2022). The approximation yields:

$$\tau = \frac{\pi}{2\omega} + i\frac{\omega_{mn}\sqrt{2}}{4Fz}. \tag{6}$$

By substituting Eqs. (5) and (6) into Eq. (1), one can calculate the transition amplitude at the point τ as:

$$A_{mn} = \mathrm{Exp}\left[i\frac{\left(2F\pi z + i\sqrt{2}\omega\omega_{mn}\right)\left(2F^2z^2 + {\omega_{mn}}^2\right) - 4F^3z^3\mathrm{Sin}\left[\frac{i{\omega_{mn}}^3}{zF\sqrt{2}}\right]}{4Fz\omega}\right]. \tag{7}$$

This complex expression integrates the effects of the electric field's strength, the frequency of the laser, and the intrinsic properties of the atomic system.

Finally, the ionization rate, W_{mn}, encapsulates the probability per unit time for the transition between states n and m. By incorporating Eq. (7) into formula for W_{mn} (see Eq. (2)) and applying a Maclaurin expansion for the sine function, $\mathrm{Sin}[x] \approx x$, when $x \to 0$ (GUO *et al.*, 2022), we obtain:

$$W_{mn} = |A_{mn}|^2 = \mathrm{Exp}\left[-2\left(\frac{\pi F^2 z^2}{\omega} + \frac{\pi {\omega_{mn}}^2}{2\omega} - \frac{{\omega_{mn}}^3}{2\sqrt{2}Fz}\right)\right], \quad (8)$$

This equation ties together the parameters governing the system's dynamics, offering a direct pathway to quantifying the transition rate in terms of measurable quantities like the field strength, F, the charge, z, laser frequency, ω, and the transition frequency, ω_{mn}. Specifically, for the Ne atom transitions $3s_2 \rightarrow 2p_4$ and $3s_3 \rightarrow 2p_5$, with transition frequencies of 6328.2 Å and 6313.7 Å respectively (LILLY and HOLMES, 1968), this formulation allows for a precise calculation of ionization rates, shedding light on the impact of laser intensity and frequency on atomic excitation processes. The consideration of these specific transitions, chosen due to their sensitivity to electron correlations and minimal relativistic effects, underscores neon's suitability as a testbed for exploring fundamental aspects of quantum dynamics and electron interaction effects in atomic systems.

RESULTS AND DISCUSSION

In this section, we present the findings from our study on the $3s_2 \rightarrow 2p_4$ and $3s_3 \rightarrow 2p_5$ transitions in Ne, employing the adiabatic Landau-Dykhne approximation (DYKHNE, 1962) as our analytical cornerstone. Our investigation meticulously explores the ionization rate W_{mn}, which is given in arbitrary units (as shown in Figs. 2-4), focusing on its sensitivity to an array of laser field intensities, I - from the relatively modest $0.01\ \mathrm{PW/cm^2}$ up to the more intense $1.00\ \mathrm{PW/cm^2}$ - alongside a spectrum of atomic charges z varying from 1 to 5, and a comprehensive range of laser wavelengths, λ, from 100 nm to 1100 nm. Anchored in the realm of atomic units, our approach provides an insightful examination of the fundamental interactions at play within the laser-atom interface, highlighting the dynamics that drive these specific Ne transitions.

First, we focus on the transition rates, W_{mn} (see Eq. (8)), for neon's $3s_2 \rightarrow 2p_4$ and $3s_3 \rightarrow 2p_5$ under diverse laser intensities, I, and atomic charges, z. The adiabatic Landau-Dykhne approximation provides a sophisticated perspective on how these parameters influence the atomic ionization processes. Presented herein are graphical representations that distill the essence of our theoretical insights into observable trends. These plots chart the course of the ionization rate's response to a sweeping range of laser intensities, from $0.01\ \mathrm{PW/cm^2}$ to an intense $1.00\ \mathrm{PW/cm^2}$. Fig. 2 presents a comparative analysis across three distinct scenarios: the comparison of ionization rates (under various laser intensities) for both transitions of interest at a single atomic charge (Fig. 2(a)), the behavior of the ionization rate for the $3s_2 \rightarrow 2p_4$ transition across a range of atomic charges (Fig. 2(b)), and a similar examination for the $3s_3 \rightarrow 2p_5$ transition (Fig. 2(c)). Understanding this dependency is crucial, not merely for the sake of theoretical completeness but also for its practical implications. The interplay presented by these graphs not only substantiates the theoretical model but also underscores the importance of parameter control in experimental setups. By elucidating the effects of laser intensity and atomic charge, we not only enhance our comprehension of neon's atomic structure but also contribute to the broader understanding of atomic behavior under extreme conditions.

As one can conclude from the results presented in Fig. 2(a), the comparison of ionization rates between the $3s_2 \rightarrow 2p_4$ (brown solid line) and $3s_3 \rightarrow 2p_5$ (brown dashed line) transitions at a constant atomic charge $z = 1$ unfolds a narrative that is corroborated by existing research (BECKER *et al.*, 2001). The brown solid line illustrates a characteristic saturation behavior as the laser intensity reaches higher values, echoing the predictions of strong-field ionization theories (PERELOMOV *et al.*, 1966; AMMOSOV *et al.*, 1986; MAJETY and SCRINZI, 2015). The brown dashed line, while following a similar trend, delineates a subtly distinct trajectory, indicative of

the delicate interplay between the atomic charge distribution and the external electric field's influence on electron ejection.

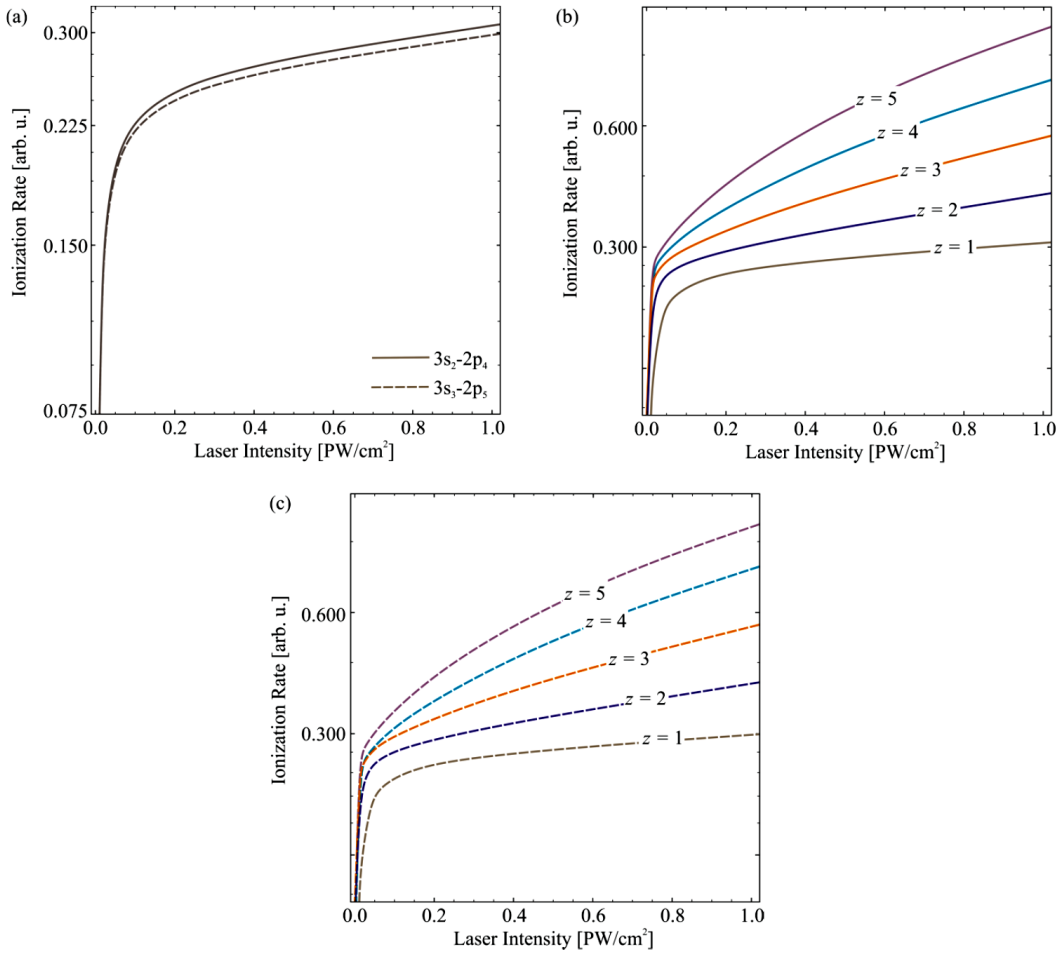

Figure 2. Variation in ionization rate, W_{mn}, as a function of laser intensity I from 0.01 to 1.00 $\mathrm{PW/cm^2}$, across distinct atomic charges z, for key Ne atom transitions. (a) Compares the ionization rates for the transition $3s_2 \rightarrow 2p_4$ (brown solid line) with the $3s_3 \rightarrow 2p_5$ transition (brown dashed line) at a constant atomic charge $z = 1$, (b) examines the $3s_2 \rightarrow 2p_4$ transition's ionization rate across atomic charges 1, 2, 3, 4, and 5, (c) analyzes the $3s_3 \rightarrow 2p_5$ transition under the same range of atomic charges.

Furthermore, Figs. 2(b), (c) extend this analysis across a wider spectrum of atomic charges z, from 1 to 5. Here, with the blue line, $z = 2$, orange line, $z = 3$, cyan line, $z = 4$, and purple line $z = 5$, each increment in atomic charge elucidates a shift in the ionization threshold and efficiency. This is completely consistent with the theoretical model that describes the scaling of ionization rates with effective nuclear charge (RISTIĆ and STEVANOVIĆ, 2007). Fig. 2(b), depicting the $3s_2 \rightarrow 2p_4$ transition across varying z, shows a systematic increase in ionization propensity with the atomic charge - a trend that has been well-documented (RISTIĆ and STEVANOVIĆ, 2007). In addition, Fig. 2(c) offers a complementary view for the $3s_3 \rightarrow 2p_5$ transition, providing a comparative perspective on the charge dependency for this distinct electronic transition. Notably, the behavior across different charges for both transitions showcases a non-linear increase in ionization rate, potentially pointing to a more complex interaction between the laser field and the multi-electron structure of Ne beyond a simplistic linear Stark effect (MAJETY and SCRINZI, 2015). This nuanced understanding of ionization dynamics, as a function of both intensity and atomic charge, is not only critical for the advancement of laser-driven applications but also for a deeper insight into the fundamental

processes governing atomic ionization. In essence, the data presented in Fig. 2 not only confirm the theoretical predictions made in this paper but also enrich our understanding of the atomic-scale phenomena underpinning ionization.

Building on the compelling narrative from Fig. 2, which highlighted the saturation behavior and the charge dependence of ionization rates, Fig. 3 aims to broaden our understanding of these phenomena across an extended parameter space. In Fig. 3(a), we dissect the behavior of ionization rates, W_{mn}, at a constant laser intensity, $I = 0.01\ \mathrm{PW/cm^2}$, for the two Ne transitions $3s_2 \rightarrow 2p_4$ (brown solid line) and $3s_3 \rightarrow 2p_5$ (brown dashed line), which may offer insights into the selection rules and electronic structures unique to each transition.

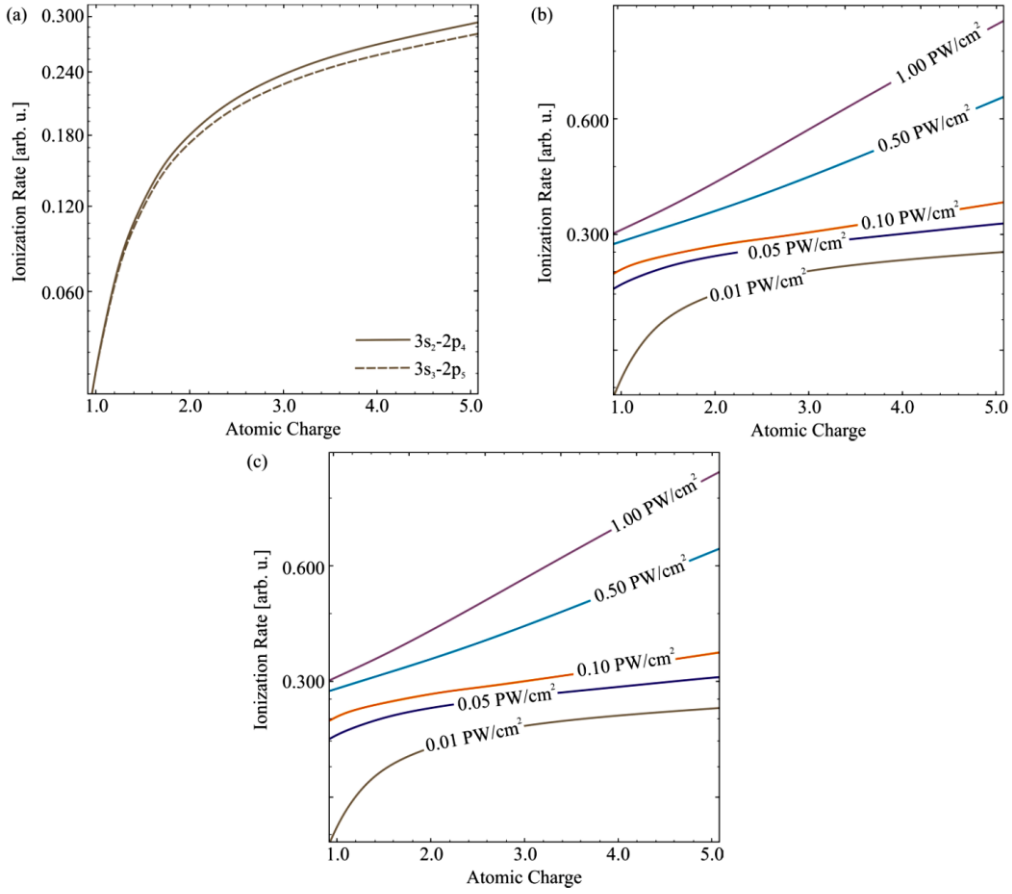

Figure 3. Variation in ionization rate, W_{mn}, as a function of atomic charges z from 1 to 5, across distinct laser intensities I, for key Ne atom transitions. (a) Compares the ionization rates for the transition $3s_2 \rightarrow 2p_4$ (brown solid line) with the $3s_3 \rightarrow 2p_5$ transition (brown dashed line) at a constant laser intensity $I = 0.01\ \mathrm{PW/cm^2}$, (b) examines the $3s_2 \rightarrow 2p_4$ transition's ionization rate across different laser intensities, $0.01\ \mathrm{PW/cm^2}$, $0.05\ \mathrm{PW/cm^2}$, $0.10\ \mathrm{PW/cm^2}$, $0.5\ \mathrm{PW/cm^2}$ and $1.00\ \mathrm{PW/cm^2}$, (c) analyzes the $3s_3 \rightarrow 2p_5$ transition under the same range of laser intensities.

Figs. 3(b) and (c) extend the scope to encompass a dynamic range of laser intensities $I = 0.01 - 1.00\ \mathrm{PW/cm^2}$, providing a comparative analysis that underscores the versatility of Ne as a probe for strong-field physics. This comprehensive examination of ionization rates serves not only to corroborate the predictions from the Landau-Dykhne model but also to shed light on the broader implications of these findings. It reinforces the necessity of precise control over experimental parameters and deepens our understanding of the quantum mechanical principles that govern ionization under intense fields. The insights gleaned from these studies are poised to inform future investigations, guiding the strategic design of experiments and the

interpretation of their results in the pursuit of advancing our command over ionization processes.

Fig. 3 provides a quantitative representation of how ionization rates, W_{mn}, evolve as a function of atomic charges z across distinct laser intensities I for the neon transitions $3s_2 \rightarrow 2p_4$ and $3s_3 \rightarrow 2p_5$. The data portrays a clear trend: as the laser intensity escalates, so does the ionization rate, yet this increase is not uniform across different atomic charges. The solid and dashed lines for $I = 0.01$ PW/cm^2 in Fig. 3(a) start to diverge as the atomic charge increases, revealing how the $3s_2 \rightarrow 2p_4$ transition responds differently compared to $3s_3 \rightarrow 2p_5$. This divergence, particularly noticeable for higher values of z, reveals the complex influence of atomic charge on ionization dynamics. The higher the atomic charge, the greater the effective nuclear attraction on the electron cloud, which in turn alters the ionization potential of the atom. Furthermore, Figs. 3(b), (c) extend the study to a broader range of intensities, showing a more pronounced increase in ionization rates for higher atomic charges. Here we observe that at the lowest intensity of 0.01 PW/cm^2 (brown line), the ionization rate for both transitions begins at its minimal value. As the intensity augments to 0.05 PW/cm^2 (blue line), the rates rise, following the established theory that higher fields correlate with an increased probability of ionization events (RISTIĆ and STEVANOVIĆ, 2007). This trend continues as we examine higher intensities of 0.10 PW/cm^2 (orange line), 0.50 PW/cm^2 (cyan line), and up to 1.00 PW/cm^2 (purple line), with each line representing an incremental step in intensity and a corresponding increase in ionization rate. This behavior aligns with quantum mechanical principles, where an increase in effective nuclear charge leads to a decrease in ionization potential, thus requiring less energy to liberate an electron (ZHAN *et al.*, 2003). The data across the various intensities and atomic charges underscore the relationship between the external laser field and the internal electronic structure of Ne atom.

Moving beyond the primary effects of laser intensity and atomic charge on ionization rates, we now turn our attention to the role of laser wavelength, λ - a parameter of critical significance in tailoring electron dynamics during ionization. Fig. 4 is dedicated to elucidating the dependence of the ionization rate W_{mn} for the transition $3s_2 \rightarrow 2p_4$ on the laser wavelength λ within the range of 100 to 1100 nm, across a series of atomic charges z for Ne (brown line $z = 1$, blue line, $z = 2$, orange line, $z = 3$, cyan line, $z = 4$, and purple line $z = 5$). A thorough comprehension of this wavelength dependency is pivotal for several reasons. Firstly, the laser wavelength directly influences the electric field's oscillation period, which in turn dictates the timescale over which the electron can respond to the field - a key factor in strong-field ionization regimes where tunneling ionization prevails. The ability to predict how ionization rates vary with laser wavelength is indispensable for the precise control of this ionization mechanism. Fig. 4 systematically explores this dependency at fixed laser intensities, providing a rich dataset to analyze how atomic ionization adapts to varying electromagnetic field conditions. In panel (a), we observe the ionization behavior at a lower intensity $I = 0.01$ PW/cm^2, serving as a foundational comparison point for the panels (b) and (c), which address moderate $I = 0.10$ PW/cm^{2}and high $I = 1.00$ PW/cm^2 laser intensities, respectively. Each panel offers a distinct glimpse into the ionization rate's sensitivity to wavelength variations, which is crucial for understanding the energy absorption process within the atom and the subsequent electron release. This aspect of wavelength dependence is especially relevant in the design of laser systems for applications such as attosecond pulse generation and high-harmonic generation, where control over the phase and amplitude of the laser-electron interaction is paramount. Moreover, the knowledge of how ionization rates vary with wavelength can significantly impact the development of laser-induced breakdown spectroscopy phenomena, enabling more accurate and controlled analysis of observed materials.

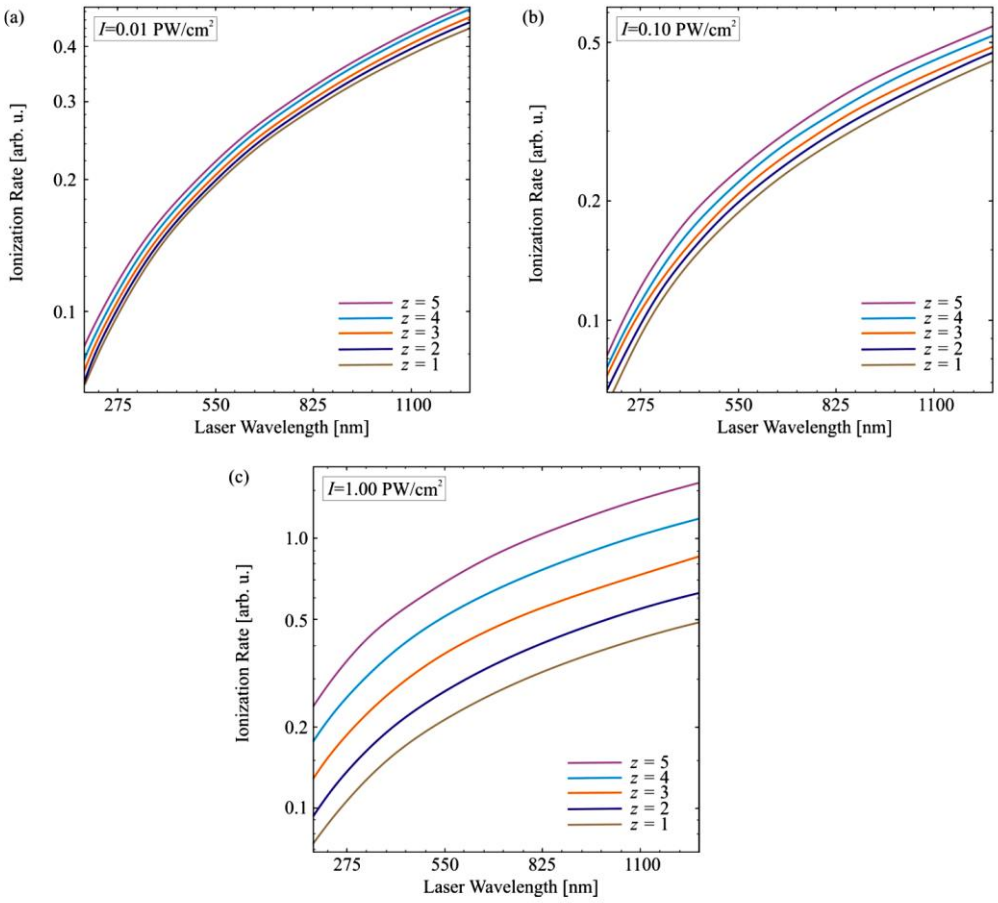

Figure 4. Variation in ionization rate, W_{mn}, for the transition $3s_2 \rightarrow 2p_4$ as a function of laser wavelength λ from 100 to 1100 nm, across distinct atomic charges z, for key Ne atom transitions. Each panel represents a different fixed laser intensity, I, and details how the ionization rate changes across a range of z: (a) demonstrates the ionization rate at a low laser intensity of $I = 0.01$ PW/cm^2 for atomic charges 1, 2, 3, 4, and 5; (b) depicts the ionization rate at a moderate laser intensity of $I = 0.10$ PW/cm^2, again for charges 1, 2, 3, 4, and 5; and (c) shows the ionization rate at a high laser intensity of $I = 1.00$ PW/cm^2 for the same range of atomic charges.

Fig. 4(a) displays the ionization rate at the lowest considered intensity, $I = 0.01$ PW/cm^2, for atomic charges $z = 1$ to $z = 5$, depicted by brown through purple lines, respectively. At this lower intensity, the energy per photon is insufficient to induce ionization via tunneling, and thus, the ionization rate is low across the entire range of wavelengths. As the wavelength increases, we do not observe a significant change in the ionization rate for any charge state, suggesting that at this lower intensity, the electron dynamics are not strongly perturbed by the variation in the laser field oscillation period. In Fig. 4(b), at a moderate intensity of $I = 0.10$ PW/cm^2, we begin to see a more discernible variation in the ionization rate with wavelength and atomic charges. This can be attributed to the increased energy per photon, which allows for the excitation and subsequent ionization of the electron, a process that becomes more efficient as the wavelength decreases and the photon energy increases (BERTOLINO *et al.*, 2020). This observation is consistent with the established understanding that shorter wavelengths can facilitate stronger electron-field interactions due to the higher photon energies involved. Furthermore, Fig. 4(c) captures the behavior at a high intensity of $I = 1.00$ PW/cm^2, where the ionization rate markedly increases across all wavelengths for each atomic charge state. This regime is where tunneling ionization becomes a dominant mechanism, and the ionization rate's dependence on wavelength becomes particularly pronounced. At shorter wavelengths, the increase in photon energy significantly boosts the ionization rate, while

at longer wavelengths, despite the intense field, the energy per photon may be below the ionization potential, leading to a lower ionization rate. Understanding the intricate dependence of ionization rates on both laser wavelength and atomic charge has profound implications. It informs the design of laser systems for precise electron dynamics control, critical in applications such as attosecond pulse generation, where the timing of electron release must be manipulated with extreme precision. Furthermore, these insights are invaluable for tailoring the wavelength of lasers used in high-harmonic generation, where ionization rates must be optimized for efficient conversion to higher frequencies. Lastly, the ability to predict and control ionization rates across a spectrum of laser wavelengths and atomic charges is pivotal for enhancing the resolution and sensitivity of laser-induced breakdown spectroscopy, enabling the accurate characterization of materials and detection of trace elements.

CONCLUSION

In conclusion, our comprehensive study has systematically elucidated the ionization dynamics of the Ne atom, particularly within the $3s_2 \rightarrow 2p_4$ and $3s_3 \rightarrow 2p_5$ transitions. Employing the adiabatic Landau-Dykhne approximation, we have quantified the ionization rate across a broad spectrum of laser intensities and atomic charges and extended our investigation to encompass the influential role of laser wavelength. Our findings illustrate a complex dependency of the ionization rate on laser intensity, atomic charge, and wavelength. At low intensities, the ionization rate remains relatively insensitive to the variations in wavelength, indicating that other factors dominate the ionization process. As the intensity increases, we observe a pronounced influence of both atomic charge and wavelength on the ionization dynamics, indicative of the transition from a regime where the field strength is paramount to one where the photon energy becomes increasingly significant. The non-linear increase in ionization rates with atomic charge, particularly notable at higher laser intensities, underscores the importance of electron-nuclear interactions and the potential barriers within the atom. These findings are consistent with and extend existing theoretical models, offering new insights into the nuanced physics governing strong-field ionization. Practically, this study's insights have significant implications for the advancement of laser-driven applications. The precise control over ionization that these findings suggest is crucial for optimizing processes in high-precision spectroscopy, advancing the frontiers of attosecond physics, and enhancing the capabilities of laser-induced breakdown spectroscopy. These applications rely on a detailed understanding of how atomic systems respond to laser fields, a topic to which our study makes a substantial contribution.

Acknowledgments

Authors would like to acknowledge the support received from the Science Fund of the Republic of Serbia, #GRANT 6821, Atoms and (bio)molecules-dynamics and collisional processes on short time scale—ATMOLCOL. Our appreciation also goes to the Serbian Ministry of Education, Science and Technological Development (Agreement No. 451-03-66/2024-03/ 200122).

References:

[1] AMMOSOV, M.V., DELONE, N.B., KRAINOV, V.P. (1986): Tunnel ionization of complex atoms and of atomic ions in an alternating electromagnetic field. *Soviet Journal of Experimental and Theoretical Physics* **64** (6): 1191.

[2] AUGST, S., MEYERHOFER, D.D., STRICKLAND, D., CHIN, S.L. (1991): Laser ionization of noble gases by Coulomb-barrier suppression. *JOSA B* **8** (4): 858–867. doi: 10.1364/JOSAB.8.000858

[3] BECKER, A., PLAJA, L., MORENO, P., NURHUDA, M., FAISAL, F.H.M. (2001): Total ionization rates and ion yields of atoms at nonperturbative laser intensities. *Physical Review A* **64** (2): 023408. doi: 10.1103/PhysRevA.64.023408

[4] BERTOLINO, M., BUSTO, D., ZAPATA, F., DAHLSTRÖM, J.M. (2020): Propensity rules and interference effects in laser-assisted photoionization of helium and neon. *Journal of Physics B: Atomic, Molecular and Optical Physics* **53** (14): 144002. doi: 10.1088/1361-6455/ab84c4

[5] BORREGO-VARILLAS, R., LUCCHINI, M., NISOLI, M. (2022): Attosecond spectroscopy for the investigation of ultrafast dynamics in atomic, molecular, and solid-state physics. *Reports on Progress in Physics* **85** (6): 066401. doi: 10.1088/1361-6633/ac5e7f

[6] DELIBASIC, H., PETROVIC, V., PETROVIC, I. (2020): Laser breakdown in water induced by λ=532nm nanosecond pulses: Analytical calculation of the number density of free electrons. *Journal of the Physical Society of Japan* **89** (11): 114501. doi: 10.7566/JPSJ.89.114501

[7] DELONE, N.B., KRAINOV, V.P. (1998): Tunneling and barrier-suppression ionization of atoms and ions in a laser radiation field. *Physics-Uspekhi* **41** (5): 469. doi: 10.1070/PU1998v041n05ABEH000393

[8] DYKHNE, A.M. (1962): Adiabatic perturbation of discrete spectrum states. *Soviet physics JETP* **14** (941): 1–13.

[9] GUO, B.N., LIM, D., QI, F. (2022): Maclaurin's series expansions for positive integer powers of inverse (hyperbolic) sine and tangent functions, closed-form formula of specific partial Bell polynomials, and series representation of generalized logsine function. *Applicable Analysis and Discrete Mathematics* **16** (2): 427–466. doi: 10.2298/AADM210401017G

[10] KELDYSH, L.V. (1965): Ionization in the field of a strong electromagnetic wave. *Soviet physics JETP* **20**: 1307.

[11] LANDAU, L.D., LIFSHITZ, E.M. (2013): Quantum mechanics: non-relativistic theory (Vol. 3). Elsevier.

[12] LILLY, R.A., HOLMES, J.R. (1968): Neon transition probabilities. *JOSA* **58** (10): 1406–1409.

[13] MAJETY, V.P., SCRINZI, A. (2015): Static field ionization rates for multi-electron atoms and small molecules. *Journal of Physics B: Atomic, Molecular and Optical Physics* **48** (24): 245603. doi: 10.1088/0953-4075/48/24/245603

[14] MILOŠEVIĆ, D.B., FETIĆ, B., RANITOVIC, P. (2022): High-order above-threshold ionization from a coherent superposition of states. *Physical Review A* **106** (1): 013109. doi: 10.1103/PhysRevA.106.013109

[15] PERELOMOV, A.M., POPOV, V.S. TERENT'EV, M.V. (1966): Ionization of atoms in an alternating electric field. *Soviet physics JETP* **23** (5): 924–934.

[16] PETERS, M.B., MAJETY, V.P., EMMANOUILIDOU, A. (2021): Triple ionization and frustrated triple ionization in triatomic molecules driven by intense laser fields. *Physical Review A* **103** (4): 043109. doi: 10.1103/PhysRevA.103.043109

[17] PETROVIĆ, V.M., MARKOVIĆ, H.S.D., PETROVIĆ, I.D. (2023): Ionization rate in an elliptically polarized laser field with respect to momentum at the tunneling exit point for noble atoms. *Results in Physics* **53**: 107005. doi: 10.1016/j.rinp.2023.107005

[18] RISTIĆ, V.M., STEVANOVIĆ, J.M. (2007): Transition rate dependence on the atom charge states, Z. *Laser Physics Letters* **4** (5): 354. doi: 10.1002/LAPL.200610124

[19] TSIBIDIS, G.D., STRATAKIS, E. (2020): Ionisation processes and laser induced periodic surface structures in dielectrics with mid-infrared femtosecond laser pulses. *Scientific Reports* **10** (1): 8675. doi: 10.1038/s41598-020-65613-w

[20] ZHAN, C.G., NICHOLS, J.A., DIXON, D.A. (2003): Ionization potential, electron affinity, electronegativity, hardness, and electron excitation energy: molecular properties from density functional theory orbital energies. *The Journal of Physical Chemistry A* **107** (20): 4184–4195. doi: 10.1021/jp0225774

[21] ZHANG, L., YANG, Y. (2020): Optimally enhanced optical emission in laser-induced breakdown spectroscopy by combining a cylindrical cavity confinement and Au-Nanoparticles action. *Optik* **220**: 165129. doi: 10.1364/OE.20.001436